APPLIED COMPUTING, MATHEMATICS AND STATISTICS GROUP
Division of Applied Management and Computing

Quasi 3-D Moment Method for Rapid Calculation of Electric Field Distribution in a Low Loss Inhomogeneous Dielectric

Ian M. Woodhead, Graeme D. Buchan and Don Kulasiri

Research Report No:99/12
August 1999

ISSN 1174-6696

RESEARCH REPORT

LINCOLN UNIVERSITY
Te Whare Wānaka O Aoraki

Applied Computing, Mathematics and Statistics

The Applied Computing, Mathematics and Statistics Group (ACMS) comprises staff of the Applied Management and Computing Division at Lincoln University whose research and teaching interests are in computing and quantitative disciplines. Previously this group was the academic section of the Centre for Computing and Biometrics at Lincoln University.

The group teaches subjects leading to a Bachelor of Applied Computing degree and a computing major in the Bachelor of Commerce and Management. In addition, it contributes computing, statistics and mathematics subjects to a wide range of other Lincoln University degrees. In particular students can take a computing and mathematics major in the BSc.

The ACMS group is strongly involved in postgraduate teaching leading to honours, masters and PhD degrees. Research interests are in modelling and simulation, applied statistics, end user computing, computer assisted learning, aspects of computer networking, geometric modelling and visualisation.

Research Reports

Every paper appearing in this series has undergone editorial review within the ACMS group. The editorial panel is selected by an editor who is appointed by the Chair of the Applied Management and Computing Division Research Committee.

The views expressed in this paper are not necessarily the same as those held by members of the editorial panel. The accuracy of the information presented in this paper is the sole responsibility of the authors.

This series is a continuation of the series "Centre for Computing and Biometrics Research Report" ISSN 1173-8405.

Copyright

Correspondence

This paper represents work to date and may not necessarily form the basis for the authors' final conclusions relating to this topic. It is likely, however, that the paper will appear in some form in a journal or in conference proceedings in the near future. The authors would be pleased to receive correspondence in connection with any of the issues raised in this paper. Please contact the authors either by email or by writing to the address below.

Any correspondence concerning the series should be sent to:

The Editor
Applied Computing, Mathematics and Statistics Group
Applied Management and Computing Division
PO Box 84
Lincoln University
Canterbury
NEW ZEALAND

Email: computing@lincoln.ac.nz

Quasi 3-D Moment Method for Rapid Calculation of Electric Field Distribution in a Low Loss Inhomogeneous Dielectric

Ian M Woodhead, Graeme D Buchan, and Don Kulasiri

Abstract – **Numerous applications of dielectric modelling require computation of the distribution of the total electric field in an inhomogeneous dielectric, in response to an applied electric field. An integral equation method would normally use an electric field volume integral technique using the moment method and hence compute the field in three-dimensional space. For those instances where the third dimension of the region is invariant, the heavy resource use of calculating the additional dimension is an unnecessary burden. The revised method reported in this paper sums the field contribution from the invariant third dimension at each stage of the two dimensional calculation, reducing the order of the model matrix by $4n^2$ where n is the number of cells in each dimension. Thus by accepting a small loss in accuracy of less than 3%, this procedure reduces the required memory resource by more than $4n^2$, and execution time is dramatically improved. Assuming an essentially lossless permittivity, we use the calculated electric field distribution from a parallel transmission line to calculate the line's propagation velocity, and demonstrate favourable comparison with measured values.**

I. INTRODUCTION

Static or quasi-static dielectric modelling may be defined as the determination of the resultant electric field strength in arbitrary low-loss dielectric media, given some incident or impressed field. The impressed field may be known, or calculated from a given array of conducting bodies with known potentials or charge distributions. Two commonly used methods for solving the inhomogeneous dielectric problem are differential equation (DE) methods that include finite difference and its commonly used derivative the finite element method, and integral equation (IE) techniques such as the method of moments. Finite element methods for this class of problem are fast and applicable to two dimensions, but often require the calculations to extend beyond the region of interest, to cover the entire domain of the problem. This generally means calculating to a boundary selected so that the influence of the boundary field on the result is considered negligible, and then imposing boundary conditions (typically Dirichlet). IE methods are well suited to applications where the region of interest is bounded by free space, since under these circumstances, calculations need only be performed inside the anomalous region, hence reducing the scale of the problem. Further, where the impressed field is altered in amplitude, position or distribution, the matrix that forms the system of equations is unchanged. Even when the electrical properties of the medium are altered, only some components of the matrix are affected; the others are dependent only on the geometry of the anomalous region. These features have a significant benefit if the modelling forms part of tomographic inversion, where the calculation is repeated using the same physical properties of the region, but with an altered impressed field. However, a significant disadvantage of IE methods for the inhomogeneous dielectric class of problem is that they require a volume integral approach and hence calculation in three dimensions, even if there is invariance in one direction. Also, the matrix is full compared with the sparse, usually banded (though larger) matrix typical of differential equation approaches [1].

Our development of the technique is a precursor to our development of dielectric tomography using an open, balanced transmission line, positioned over a half-space composite medium. In this case, the dielectric region is bounded by free space, suggesting the appropriateness of an integral equation method. Here we describe the use of a moment method [2], tailored to the particular characteristics desirable for such a tomographic forward solution. The region is discretised to appropriately shaped elements or cells, and the polarisation is represented by a single dipole at the centre of each cell. The field in each cell is the vector sum of the impressed field and the individual electric field contributions from every dipole in the anomalous region. Model accuracy is governed by the extent or graininess of the discretisation, and the accuracy of representing the polarisation field in the cell by a dipole at its centre. Cell discretisation also affects the discretisation of the impressed field, so where the field has a strong gradient, accuracy is usefully improved by reducing cell size, but at the expense of increased execution time. By more accurately integrating the field over the area of each cell, the time required to calculate the field in each cell is likely to increase. However, this may well be more than compensated for by the increased granularity that may then be tolerated [3]. The approach described here employs the commonly used pulse basis functions, although alternative methods that do not impose field uniformity in each cell may further enhance accuracy in zones of high contrast.

The method described here relates to a static or quasi-static field, and in this case is the field surrounding a parallel transmission line where the axial field is considered zero. This contrasts with alternative treatments such as [4] and [3] where the electric field is unguided, and thus scattering in the direction of the Poynting vector nullifies the validity of a pseudo static approach.

In this paper we first justify the use of the pseudo-static approach for low loss transverse electromagnetic mode (TEM) propagation, then demonstrate the moment method and calculation of propagation velocity for the case of a parallel transmission line embedded in a laterally inhomogeneous permittivity distribution. Different discretisation or integration schemes will not be explored. Next, the pseudo 3-D technique will be described, compared with the full 3-D method, and finally verified by comparing predicted and measured propagation velocities

II. JUSTIFICATION FOR THE USE OF QUASI-STATIC TECHNIQUES WHEN MODELLING TEM PROPAGATION

Assuming that the quantities ε, σ and μ are independent of time, the two Maxwell equations that describe electromagnetic wave propagation may be written as

$$\nabla \times E = -\mu \frac{\partial H}{\partial t} \quad (1)$$

$$\nabla \times H = \sigma E + \varepsilon \frac{\partial E}{\partial t} \quad (2)$$

The right hand side of Eqn 2 comprises the conduction current due to the conductivity σ of the propagating medium, and the displacement current due to the energy storage or real component ε, of the permittivity.

Now consider TEM propagation along a parallel transmission line, where the transverse plane is described by the x and y Cartesian coordinates and the longitudinal coordinate is z. Then in the case of a guided electromagnetic wave propagating with zero loss, the z component of both E and H is zero. Then considering the x-z plane, it may be shown [5] that

$$\frac{\partial^2 E_x}{\partial z^2} = \mu\varepsilon \frac{\partial^2 E_x}{\partial t^2} \tag{3}$$

Solutions of Eqn 3, the one-dimensional wave equation, lie on characteristic curves [6] defined by

$$\frac{dz}{dt} = \frac{1}{\sqrt{\mu\varepsilon}} \tag{4}$$

The propagation velocity v defined by Eqn 4, is independent of the rate of change of E with respect to time, and hence independent of the slope of a voltage pulse, or equivalently its frequency spectrum as represented by a Fourier series.

We now turn to the case where the medium has a small loss. Provided the loss is sufficiently small that $\sigma << \omega\varepsilon$ where ω is the angular frequency, the conduction current contribution in Eqn 2 may be ignored, and Eqn 3 adequately describes the wave propagation. Then the complex permittivity that incorporates the loss component ε'' is $\varepsilon' + j\varepsilon''$, and may be replaced by $\varepsilon' + j\frac{\sigma}{\omega}$. Consequently, it can be shown that the propagation velocity in the low-loss case is adequately represented by a truncated series expansion:

$$v \approx \frac{1}{\sqrt{\mu\varepsilon(1+\frac{\sigma^2}{8\varepsilon^2\omega^2})}} \qquad (5)$$

Returning to our earlier assumption on loss, it may be shown [5] that even when considering the skin effect resistance of a parallel transmission line, the real or loss component (resistance) within the conductor is small compared with the imaginary or inductive component (i.e. $R << \omega L$ where R and L are respectively the distributed resistance and inductance per unit length of the transmission line). The axial or longitudinal component of the magnetic field will be small if the loss within the medium is also small. This condition will be met if $G << \omega C$ where G and C are respectively the distributed conductance and capacitance per unit length, or in the terminology of Eqn 2 by the condition that $\sigma << \omega\varepsilon$. This is equivalent to $\sigma << 0.6$ S/m in a typical TDR measurement situation where the frequency component that is measured is 1 GHz, and ε_r of the material surrounding the transmission line is 10, representing a volumetric water content of approximately 20%.

The consequence of a small axial magnetic field is that the transverse voltage thereby induced makes little contribution to the integral of *E.dl.* Similarly, a small axial electric field makes little contribution to the transverse magnetic field by the displacement current. Thus the assumption of essentially zero axial components of *E* and *H* that lead to Eqn 3 is valid.

III. TDR FOR MOISTURE CONTENT MEASUREMENT: THE 2-D CASE

The application that will follow from this work is modelling the response of a parallel transmission line influenced by a surrounding composite material that is likely to have an inhomogeneous moisture content and hence permittivity distribution. Using a suitable dielectric model of the material, the propagation velocity is a good indicator of the moisture content. The methods described here are useful for quantifying the response to laterally non-uniform moisture content. Further, [7] commented that provided the parameter of interest, in their case volumetric water content θ, had a square root relationship with permittivity ε, it would be accurately integrated in the axial direction of the transmission line. In the case of soil [7], the empirically derived $\theta(\varepsilon)$ dielectric model of [8] was dominated by the square root term. Under similar circumstances where the axial integration is near linear, an effective permittivity distribution in 2-space, may be considered equivalent to the actual inhomogeneous 3-space distribution. This facet arises since in general, a TDR system is unable to quantify axial variation. The axial integration on a lossless line may be described as follows. For a small segment of line *dl*, the propagation time t_n is

$$t_n = \frac{\sqrt{\varepsilon_n}\,dl}{k} \tag{6}$$

where v is the velocity, ε_n is the effective permittivity surrounding the line at position n, and k is a constant incorporating the permeability (assumed invariant). Then the resultant propagation time along the line is

$$t = \frac{\int_0^n \sqrt{\varepsilon_n dl}}{k} \tag{7}$$

Thus provided (and this is commonly the case) ε is proportional to the square of the volumetric moisture content θ, axial integration will be linear. Hence, a piecewise determination of the propagation velocity within each dl will provide a valid comparison with measured θ in a heterogeneous material.

IV. TDR PROPAGATION VELOCITY IN A LOSSLESS INHOMOGENEOUS DIELECTRIC

The polarisation of a discretised zone or cell within a dielectric material may be represented by a dipole at its geometric centre. In most dielectric materials, there is no net polarisation until it is imposed by an external or impressed field. When applied to this static or quasi-static electric field problem, the moment method may be considered as the summation in each cell, of the electric field contributions due to the polarisation in all other cells. Cubes are a convenient cell shape for a Cartesian coordinate system and are used here, but cells with trapezoidal [9] or hexagonal cross-sections are viable alternatives.

Given an impressed electric field $\tilde{E}_i(r)$ in a region, the total resultant electric field distribution $\tilde{E}_{tot}(r)$, for a material of arbitrary permittivity distribution $\varepsilon(r)$ is:

$$E_{tot}(r) = E_i(r) + E_{pol}(r) \quad (8)$$

$$\text{i.e.} \quad \frac{P(r)}{\varepsilon_0 \chi(r)} = E_i(r) + E_{pol}(r) \quad (9)$$

$$\text{or} \quad -E_i(r) = E_{pol}(r) - \frac{P(r)}{\varepsilon_0 \chi(r)} = K(P) \quad (10)$$

where K is a linear operator acting on the polarization P, E_i the external impressed field and $\chi(x,y,z)$ is the electric susceptibility ($\varepsilon_r(x,y,z)$ - 1). The polarisation region may now be discretised, and following the moment method [2], we calculate the matrix of polarisation vectors $P(x, y, z)$:

$$[K][P] = -[E_i] \quad (11)$$

$$\text{so} \quad [P] = -[K]^{-1}[E_i] \quad (12)$$

We next extract the electric field strengths.

$$E_{tot}(r) = \frac{P(r)}{\varepsilon_0 \chi(r)} \quad (13)$$

Finally, to complete the solution for the case of a parallel transmission line, the voltage between the lines is obtained from a line integral over a suitable integration path l between the lines, and then substituted in the telegraphers equation for a lossless line.

$$C = \frac{q}{\int \underset{\sim}{E}(r) \cdot d\underset{\sim}{l}} \tag{14}$$

$$vel = \frac{1}{\sqrt{LC}} = \sqrt{\frac{\pi}{C\mu \cosh^{-1}\left(\frac{b}{a}\right)}} \tag{15}$$

Here q is the r used to define the impressed field, C and L are respectively the capacitance and inductance per unit length of the transmission line, and a and b are respectively the diameter and spacing of the transmission line elements. To complete the solution, the value of $\underset{\sim}{E}_{pol}$ is required.

Consider the influence of a region (U) of polarised material on the potential at point f. The total polarisation of U can be represented by a dipole at the centre of the region, and with dipole moment $\underset{\sim}{P}$ (Fig. 1).

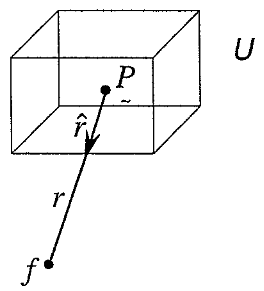

Fig. 1. Geometry of a region of polarisation.

From electrostatic theory, the potential at f is [10]:

$$\phi_f = \frac{1}{4\pi\varepsilon_0}\frac{\underset{\sim}{P}.\hat{r}}{r^2} = \frac{1}{4\pi\varepsilon_0}\frac{\underset{\sim}{P}.\underset{\sim}{r}}{r^3} \tag{16}$$

where $\hat{r}$ is a unit vector pointing to f.

The electric field is $E_f = -grad\phi_f$ where for Cartesian coordinates, $\nabla\phi = \hat{x}\phi_x + \hat{y}\phi_y + \hat{z}\phi_z$.

Since, $\frac{dr}{dx} = \frac{x}{r}$ and $\underset{\sim}{x} = x\hat{x}$,

$$\phi_x = \frac{\underset{\sim}{P}.}{4\pi\varepsilon_0 r^5}\left(\hat{x}(r^2 - 3x^2) - \hat{y}.3xy - \hat{z}.3xz\right) \tag{17}$$

Similar expressions are obtained for ϕ_y and ϕ_z, so that in dyadic form,

$$\underset{\sim}{E}_f = \frac{-\underset{\sim}{P}.}{4\pi\varepsilon_0 r^5}\begin{bmatrix} \hat{x}\hat{x}(r^2 - 3x^2) - \hat{x}\hat{y}.3xy - \hat{x}\hat{z}.3xz \\ - \hat{y}\hat{x}.3yx + \hat{y}\hat{y}(r^2 - 3y^2) - \hat{y}\hat{z}.3yz \\ - \hat{z}\hat{x}.3zx - \hat{z}\hat{y}.3zy + \hat{z}\hat{z}(r^2 - 3z^2) \end{bmatrix} \tag{18}$$

From superposition the total field at S due to all contributions is:

$$\underset{\sim}{E}_f = \int_{all\ U} -\nabla.\frac{1}{4\pi\varepsilon_0}\frac{\underset{\sim}{P}.\underset{\sim}{r}}{r^3}dv \tag{19}$$

And from the linearity of field contributions,

$$\underset{\sim}{E}_f = -\frac{1}{4\pi\varepsilon_0}\nabla\int_{all\ U}\frac{\underset{\sim}{P}.\underset{\sim}{r}}{r^3}dv \tag{20}$$

We may then discretise to obtain the required $\underset{\sim}{E}_{pol}(r)$.

$$\underset{\sim}{E}_{pol} = \underset{\sim}{E}_f = -\frac{1}{4\pi\varepsilon_0}\nabla\sum_r\frac{\underset{\sim}{P}.\underset{\sim}{r}}{r^3}\cdot\Delta v \tag{21}$$

where Δv is the volume of the region U. Matrix K in Eqn 11 contains a set of entries for each field point, and each entry corresponds to the contribution from a source point that corresponds to a region U, resulting in an $F.S$ by $F.S$ matrix where F and S are respectively the number of field and source points. Each entry comprises nine elements representing the three coordinate directions of the field, in response to the three components of the source field, nine elements in total.

V. PSEUDO 3-D METHOD

The pseudo 3-D method utilises assumed permittivity invariance in the third (z) dimension, to enable the polarisation field contributions to be summed for all z, at each x and y position. In practice, the matrix l is constructed in two dimensions, and additional field contributions are included for each entry. The added field contributions correspond to each cell that is perpendicular to the x-y plane at (x',y'), and take the same form as elements in Eqn 18.

For example, a particular value of x and y leads to the $\hat{x}\hat{x}$ component $3x^2 - r^2$ in the x-y or in this case, $z = 0$ plane (the $\hat{x}\hat{x}$ component is the field in the x direction, arising from the x-field at the source point). The additional off-plane components take the same form, but the vector $\tilde{r}$ and the common factor r^{-2}, include a z component. Hence the calculation for the field at (x,y) due to the dipole fields at (x', y'), for the five cells ranging from z = -2 units to z = +2 units, includes the geometric component:

$$\frac{\Delta v}{4\pi\varepsilon_0}\left[\frac{(3x^2 - r)}{r^5} + \frac{2(3x^2 - r_1)}{r_1^5} + \frac{2(3x^2 - r_2)}{r_2^5}\right] \qquad (22)$$

where Δv is the cell volume, $r_n = \sqrt{(x-x')^2 + (y-y')^2 + (z-z')^2}$ and n = 0 is the on-plane or $(z - z') = 0$ case, n = 1 the $(z - z') = \pm 1$ unit case, and n = 2 the $(z - z') = \pm 2$ unit case. We have the option of including as many planes with non-zero z-z', as are considered to contribute significantly to the field.

The simplification brought about by the pseudo 3-D model does impact on the accuracy of the solution. Although the impressed field in the z direction is invariant (zero z component), the source points possess small but non-zero z-fields arising from the x and y excitation. Since these particular contributions from the field components in the z direction are not accounted for by the pseudo 3-D method, they contribute to the modelling error.

In the three-dimensional model, there are nine electric field elements for each cell, representing the three-dimensional source field and the three field dimensions at the field point. Thus, the matrix is of a size $9n^3$ by $9n^3$ where n is the total number of discretised zones or cells. The pseudo 3-D method reduces the order of the matrix to $4n^2$ by $4n^2$, dramatically reducing storage requirements and calculation time. The calculation time reduction is dramatic despite the inclusion of additional calculation for the third dimension. Comparison with the full 3-D method using several different permittivity distributions indicated that by accepting the small loss in accuracy of less than 3%, this procedure reduces the required memory resource by more than $4n^2$, and execution time is dramatically improved.

VI. A COMPARISON OF THE METHODS

We evaluated the accuracy of the methods in two stages. First, the traditional 3-D and pseudo 3-D methods were compared, and then the output from the pseudo 3-D method was compared with experimental results.

For the first comparison, the traditional 3-D solution described above used a 5x5x5 matrix of cubic cells, and a non-uniform external field, as imposed by a nearby parallel transmission line. The pseudo 3-D method used a 5x5 matrix of cubic cells and included the field arising from five cells in the *z* direction. Differences in calculated electric field ranged from zero to 1.65% when comparing the results within and near a cube of relative permittivity ε_r=3. When one row of cells in the z direction was given a permittivity ε_r=1000, the maximum error (that of the field strength in the centre set of cells), rose to 2%. When implementing the procedures in Matlab Ver 4, on a 100 MHz PC with 80 MB of RAM, the maximum number of cells without apparent use of virtual memory improved from 7x7(x7) to 28x28(x28). The execution time improved from 648 seconds to 5 seconds for the 7x7(x7) problem. With each method the self-field, represented whenever the field and source cells of the moment method coincide, was calculated using $\frac{1}{2.8\varepsilon_0}$ since the approximation used in [2] resulted in numerical instability.

We chose to verify the pseudo 3-D calculation by comparison with measured propagation times for a parallel transmission line above a water-filled phantom body, using a Tektronix 1502C connected with 0.8 m of URM 43 coaxial cable to a 1:4 balun. Balun construction followed [11], but omitted the initial 1:1 transformer, and used a single, grade S3 ferrite toroid. A relay (similar to Teledyne 172) switched the balanced line to either a reference transmission line or the measuring line. The 6 mm diameter stainless steel rods were spaced 60 mm apart, with the measuring rods 300 mm longer than the reference rods. At the end of the transmission lines, 6 x 1 mm steel shorting straps were used since with the balun described above, they provided sharper, better defined reflections than unterminated lines. Waveform data retrieved from the 1502 were smoothed and differentiated using 25 point routines [12]. The intersection between the tangents to the maximum negative slope and the immediately preceding stationary point defined the edge of the pulse. Finally, the reading from the reference line was subtracted from that of the measuring line to obtain the actual travel time of the edge.

A rectangular thin walled plastic container 150 mm wide by 500 mm long by 80 mm deep filled with water formed the phantom dielectric body. The transmission line was positioned near the phantom and used computer readable position sensing with 1mm precision to record relative positions.

VII. RESULTS AND DISCUSSION

Table 1. Comparison of measured and calculated propagation times.

Position (mm)	Measured (ns)	Model (ns)	Discrepancy (ps)	Normalised (ps)
-30, 5	1.071	1.076	5	-16
-30, 10	1.016	1.039	23	2
-30, 20	1.001	1.017	18	-3
-30, 30	0.992	1.010	18	-3
45, 5	1.172	1.204	32	11
45, 10	1.047	1.103	56	35
45, 20	1.009	1.035	26	5
45, 30	0.998	1.019	21	0
distant	0.987	1.008	21	0

The position is defined as the (x, y) distances (mm) between the top edge of the container and the geometric centre of the transmission line (Fig. 2). A 'distant' separation provided a reference reading to normalise the data. Model predictions were calculated using 5 mm cubic cells and a pseudo 3-D approach that included the influence of the neighbouring cells in the *z* direction within the 2-D (*xy*) matrix. The value used for ε_r of water in the model took account of the water temperature in the container.

While we would expect model errors to be greatest when the rods were near the phantom, and hence the field gradients were large, we cannot attribute to this the repeatable discrepancy of 35 ps that occurred at a 10 mm spacing between the rods and the phantom. Consequently, we assume that small errors due to non-linearity or ripple in the time-base ramps in the 1502C [13] were responsible for the apparent measurement error. The differencing technique using the reference transmission lines was believed to remove consistent errors from the measurements, since repeatable results were obtained.

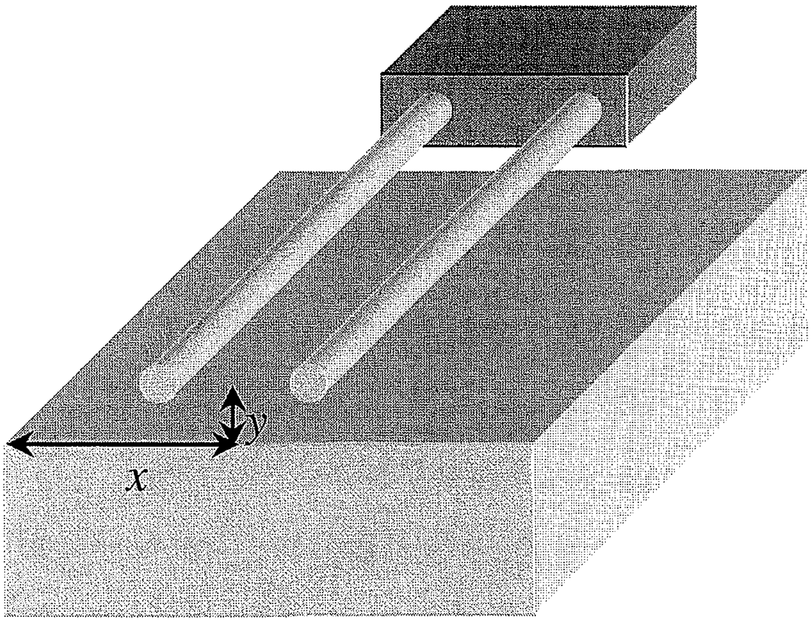

Fig. 2. Position of transmission line and phantom dielectric body.

VIII. CONCLUSIONS

We have described an IE method for determining the electric field distribution in a low loss, inhomogeneous dielectric material given a pre-determined impressed field, $\underset{\sim}{E}_i$. In the case of a parallel transmission line generating $\underset{\sim}{E}_i$, the procedure has been extended to calculate line parameters and hence the propagation velocity of a pulse on the line. Thus the procedure enables prediction of the impact of arbitrary dielectric (or moisture content) distributions on a TDR measurement system, and quantification of its sensitivity distribution. Experimental verification using water as a dielectric body provided good agreement with the model predictions. Further exploration of the small discrepancies between the model and experimental results could be achieved using higher precision TDR instrumentation.

IE methods have several advantages over DE methods when used for calculating electric field distribution, but are constrained to calculate all three-space dimensions when used with an inhomogeneous medium. Consequently, the method is computationally inefficient where a 2-D representation would otherwise suffice. We have shown above that for those applications where the third dimension is invariant, a new pseudo 3-D method demonstrates good agreement with the full 3-D method even for high permittivity contrasts (80:1). The method we have described has a dramatically smaller demand on memory and processing resources.

REFERENCES

[1] K. J. Binns, P. J. Lawrenson, C. W. Trowbridge, *The Analytical and Numerical Solution of Electric and Magnetic Fields.* Chichester: John Wiley & Sons Ltd, 1992, 470 p.

[2] R. F. Harrington (ed.), *Field Computation by Moment Methods*, 2nd ed. Molabor, Fl: R. E. Kreiger, 1987.

[3] C. Tsai, H. Massoudi, C. H. Durney, and M. F. Iskander, "A procedure for calculating fields inside arbitrarily shaped, inhomogeneous dielectric bodies using linear basis functions with the moment method," *IEEE Trans. Microwave Theory and Techniques*, vol. MTT-34, pp. 1131-1139, 1986.

[4] T. C. Guo, W. W. Guo, and H. N. Oguz, "A technique for three-dimensional dosimetry and scattering computation of vector electromagnetic fields," *IEEE Trans. Magnetics*, vol. 29, pp. 1636-1641, 1993.

[5] S. Ramo, J. R. Whinnery, and T. Van Duzer, *Fields and Waves in Communication Electronics*, 3rd ed. New York: Wiley, 1993.

[6] W. E. Williams, *Partial Differential Equations.* Oxford: Clarendon Press, 1980.

[7] P. A. Ferré, D. L. Rudolph, and R. G. Kachanoski, "Spatial averaging of water content by time domain reflectometry: Implications for twin rod probes with and without dielectric coatings," *Water Resources Research,* vol. 32, pp. 271-279, 1996.

[8] G. C. Topp, J. L. Davis, and A. P. Annan, "Electromagnetic determination of soil water content: measurements in coaxial transmission lines," *Water Resources Research*, vol. 16, pp. 574-582, 1980.

[9] D. H. Schaubert and P. M. Meaney, "Efficient computation of scattering by inhomogeneous dielectric bodies," *IEEE Trans. Antennas and Propagation*, vol. AP-34, pp. 587-592, 1986.

[10] A. F. Kip, *Fundamentals of Electricity and Magnetism*, 2nd ed. McGraw-Hill, 1962.

[11] E. J. A. Spaans and J. M. Baker, "Simple baluns in parallel probes for Time Domain Reflectometry, *Soil Sci. Soc. Am. J.* vol. 57, pp. 668-673, 1993.

[12] A. Savitsky and M. J. E. Golay, "Smoothing and differentiation of data by simplified least squares procedures," *Analytical Chemistry*, vol 36, No. 8, 1964.

[13] W. R. Hook and N. J. Livingston, "Propagation velocity errors in Time Domain Reflectometry measurements of soil water," *Soil Sci. Soc. Am. J.*, vol. 59, pp. 92-96, 1995.